Synoptic tracer gradients in the upper troposphere over central Canada during the Stratosphere-Troposphere Experiments by Aircraft Measurements 1998 summer campaign

H. Fischer,[1] D. Brunner,[2,3] G. W. Harris,[4] P. Hoor,[1] J. Lelieveld,[1] D. S. McKenna,[5,6] J. Rudolph,[4] H. A. Scheeren,[7] P. Siegmund,[2] H. Wernli,[8] J. Williams,[1] and S. Wong[1]

Received 28 December 2000; revised 18 June 2001; accepted 18 June 2001; published 24 April 2002.

[1] During the July 1998 Stratosphere-Troposphere Experiments by Aircraft Measurements (STREAM) intensive campaign, eight measurement flights were conducted from Timmins airport (Ontario, Canada, 48.2°N, 79.3°W). In situ measurements of ozone, carbon monoxide, carbon dioxide, and nonmethane hydrocarbons, as well as three-dimensional back trajectories based on European Centre for Medium-Range Weather Forecasts wind field analyses, are used to characterize upper tropospheric air masses with respect to their origin. In the upper troposphere between 8 km and the local tropopause, about 40% of the air masses originated from the subtropics/tropics south of 30°N, about 50% originated from midlatitudes (between 30° and 50°N), and 12% originated from the polar region north of 50°N. In general, highest trace gas levels were observed in air masses originating from midlatitudes (e.g., CO, 107 ± 25 ppbv; ethane, 983 ± 385 pptv; acetylene, 119 ± 43 pptv), with the exception of CO, which had highest mixing ratios (121 ± 11 ppbv) in air masses of polar origin. The lowest concentrations were generally observed in air masses of (sub)tropical origin (e.g., CO, 64 ± 2 ppbv; ethane, 424 ± 86 pptv; acetylene, 39 ± 14 pptv). For CO and most of the alkanes a significant positive latitudinal gradient was observed, while CO_2 and CH_3Cl exhibited an inverse gradient with lowest mixing ratios at high northern latitudes. This reflects the different source and sink distributions of the investigated species. Ozone mixing ratios significantly increased in the upper troposphere above 8 km altitude, at least partially because of stratosphere-troposphere exchange. Approximately 10% of the upper tropospheric air was directly influenced by recent cross-tropopause exchange. A case study indicates that the convergence of air masses of different origin along a cold front creates sharp gradients not only in temperature and humidity but also in trace gas concentrations. It is shown that these mesoscale gradients result from the organized flows of tropical, arctic, and stratospheric air masses. *INDEX TERMS:* 0300 Atmospheric Composition and Structure; 0322 Atmospheric Composition and Structure: Constituent sources and sinks; 0365 Atmospheric Composition and Structure: Troposphere—composition and chemistry; 0368 Atmospheric Composition and Structure: Troposphere—constituent transport and chemistry; *KEYWORDS:* upper troposphere, chemical composition, stratosphere-troposphere exchange, airstreams, coherent trajectory ensembles

1. Introduction

[2] The Hudson Bay lowlands in central northern and northeastern Canada constitute one of the largest natural wetlands in the world. In the summer this remote subarctic region is often influenced by air pollution as a result of regional biomass burning, long-range transport, and deep convection over the Great Lakes area [*Wofsy et al.*, 1994]. Moreover, the close proximity to the polar jet stream results in the frequent occurrence of stratospheric intrusions into the troposphere [*Bachmeier et al.*, 1994]. These complex transport patterns have a strong influence on the chemical composition of the troposphere over the lowlands, in addition to the contribution from local emissions, i.e., biogenic emissions from the tundra and combustion products from natural wildfires [*Wofsy et al.*, 1994]. Canadian forest fires not only are a source of local pollution but also have been identified as major sources of elevated CO concentrations over the southeastern United States [*Wotawa and Trainer*, 2000] and over the eastern Atlantic [*Waibel et al.*, 1999] during summertime episodes, several thousand kilometers downwind of the fires.

[3] During July–August 1990 the Arctic Boundary Layer Expedition (ABLE) 3B first characterized the chemical state of the lower and middle troposphere in this part of Canada [*Harriss et al.*, 1994a]. Since the measurement flights during ABLE 3B were performed at altitudes below 6 km, information about the upper troposphere was limited to ozone and aerosol profiles from

[1]Max Planck Institute for Chemistry, Mainz, Germany.
[2]Royal Netherlands Meteorological Institute, DeBilt, Netherlands.
[3]Now at Institute for Atmospheric Science, Eidgenossische Technische Hochschule Hönggerberg, Swiss Federal Institute of Technology, Zürich, Switzerland.
[4]Centre for Atmospheric Chemistry, York University, North York, Ontario, Canada.
[5]Forschungszentrum Jülich, Jülich, Germany.
[6]Now at National Center for Atmospheric Research, Boulder, Colorado, USA.
[7]Institute for Marine and Atmospheric Research, Utrecht University, Utrecht, Netherlands.
[8]Institute for Atmospheric Science, Eidgenossische Technische Hochschule Hönggerberg, Swiss Federal Institute of Technology, Zürich, Switzerland.

0148-0227/02/2000JD000312$09.00

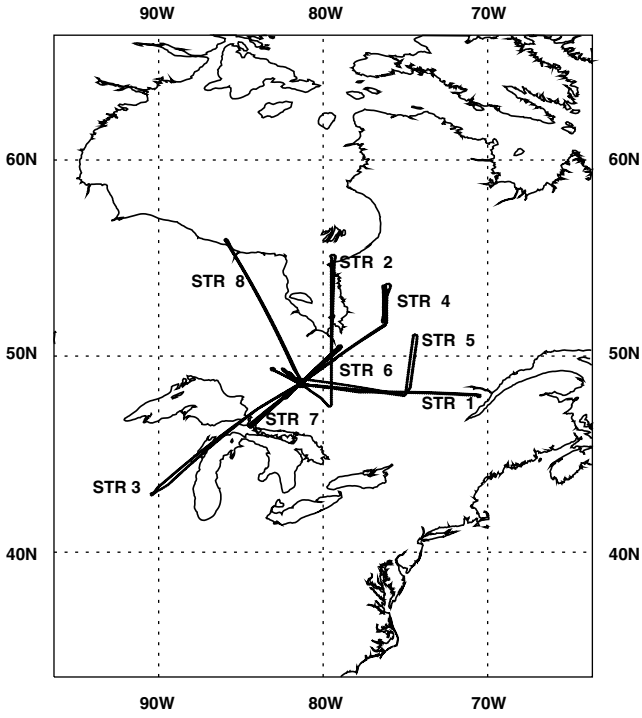

Figure 1. Flight tracks of the eight STREAM measurement flights over Ontario, Canada, from Timmins (48.2°N, 79.3°W) during July 1998.

an onboard lidar system [*Browell et al.*, 1994]. Five main factors were identified that influenced summertime O_3 concentrations: (1) stratosphere-troposphere exchange, (2) precursor emissions from biomass burning, (3) long-range transport of industrial pollution from the United States, (4) biogenic emissions, and (5) very long range transport of tropical air to northern high latitudes [*Harriss et al.*, 1994a].

[4] In July 1998 a second airborne campaign was performed over the northern part of Ontario from Timmins (48.2°N, 79.3°W) as part of the Stratosphere-Troposphere Experiments by Aircraft Measurements (STREAM) project. The aim of this STREAM campaign was to study the mechanisms that lead to transport of emission plumes from boreal fires in northern Canada and polluted boundary layer air from the Great Lakes area (urban plumes) into the upper troposphere and lowermost stratosphere and subsequent transport over the Atlantic Ocean toward Europe. Because the jet aircraft used, a Cessna Citation II, can reach a maximum altitude of 13 km, the campaign offered a unique opportunity to extend the ABLE 3B studies to the upper troposphere and lowermost stratosphere. Here we concentrate on the chemical composition of the upper troposphere, notably on carbon monoxide (CO), carbon dioxide (CO_2), nonmethane hydrocarbons (NMHC), and O_3. We focus on the chemical composition as a function of air mass origin as deduced from backward trajectories. We distinguish between tropical/subtropical, midlatitudinal, and polar air mass origin. A detailed discussion of the NO_y budget in the upper troposphere during STREAM 1998, with special emphasis on the contribution of lightning NO_x, is given by *Lange et al.* [2001]. Trace gas distributions in the lowermost stratosphere are the topic of the paper by *Hoor et al.* [2002].

2. STREAM 1998 Summer Campaign

[5] During the STREAM summer intensive campaign, eight measurement flights were conducted from Timmins airport (Ontario, Canada) in the period between 1 July 1998 and 15 July 1998 (Figure 1). The flights were performed with a Cessna Citation II jet aircraft operated by the Technical University of Delft, Netherlands. The aircraft can reach a maximum altitude of 13 km and has a range of approximately 2000 km at an average cruising speed of 150 m s^{-1}. It is equipped with instrumentation for trace gas and aerosol measurements: a tunable diode laser absorption spectroscopy (TDLAS) instrument for CO, N_2O, and CH_4 measurements [*Wienhold et al.*, 1998], an in situ gas chromatograph for CF_2Cl_2 (F12) and either N_2O or $CFCl_3$ (F11) [*Bujok et al.*, 2001], a commercial nondispersive infrared analyzer for CO_2 measurements, a Lyman-α fluorescence instrument for high-precision water vapor measurements [*Zöger et al.*, 1999], an ion-molecule reaction mass spectrometer for the detection of gas phase HNO_3 [*Möhler and Arnold*, 1991], chemiluminescence instruments for the detection of NO [*Lange et al.*, 2001], NO_y [*Fischer et al.*, 1997], and O_3 [*Bregman et al.*, 1995], and condensation particle counters for size-resolved aerosol detection in the 0.007 to 1 μm range [*Schröder and Ström*, 1997]. Besides these in situ instruments, which provide measurements at high time resolution, nine electropolished stainless steel canisters are filled per flight with pressurized ambient air, which

Table 1. Measurement Flights Performed During STREAM 1998

Flight	Date	Flight Levels, km	Location Over Canada	Objective	Air Mass Origin
STR-1	1 July 1998	10, 10.6, 11.2, 11.8, and 12.5	east of Timmins	stratospheric background	midlatitude/ polar
STR-2	3 July 1998	10, 10.6, and 11.8	north of Timmins	stratospheric background	polar
STR-3	5 July 1998	10, 10.6, and 11.8	southwest toward Lake Michigan	convective outflow	midlatitude/ tropical
STR-4	8 July 1998	10, 10.6, 11.2, 11.8, and 12.5	northeast of Timmins	convective outflow	polar
STR-5	10 July 1998	10, 11.8	east of Timmins	North Atlantic flight corridor	polar
STR-6	12 July 1998	10, 10.6, 11.2, 11.8, and 12.5	northeast of Timmins	biomass burning	midlatitude
STR-7	15 July 1998	11.2, 11.8, 12.5, and 13.1	southwest toward Lake Michigan	ahead of cold front	tropical
STR-8	15 July 1998	7.6 and 9.7	northwest toward Hudson Bay	behind cold front, tropopause fold	midlatitude/ polar

is analyzed after the campaign using gas chromatographic techniques [*Lelieveld et al.*, 1999].

[6] Table 1 lists the measurement flights performed during STREAM 1998, providing information about the date, flight levels, direction, overall objective, and main air mass origin for the individual flights. In general, the flights were planned to perform measurements in the tropopause region between 8 and approximately 12.5 km near the polar front or large-scale convective systems to study upward transport and subsequent outflow as well as cross-tropopause transport. They comprised several constant level tracks in the upper troposphere and lowermost stratosphere, either along ''stacked'' flight levels or low-level outbound and high-level inbound flights.

3. Aircraft Instrumentation

[7] The following analysis mainly relies on CO, CO_2, O_3, and NMHC measurements obtained during the eight STREAM flights. This section provides more details on the instrumentation used for these measurements.

[8] Tunable diode laser absorption spectroscopy (TDLAS) was used for the determination of N_2O, CH_4, and CO mixing ratios. The Max Planck Institute for Chemistry Tracer In Situ TDLAS for Atmospheric Research (TRISTAR) instrument, which allows the measurement of up to three atmospheric trace gases simultaneously with a time resolution of 1 s, is described in detail by *Wienhold et al.* [1998]. In situ CO, CH_4, and N_2O calibrations were performed during the flights on a regular basis by replacing the ambient air with a known secondary standard from a pressurized tank. The calibration gas standards were cross-calibrated against a primary standard before and after the campaign. Typical calibration gas concentrations for N_2O, CH_4, and CO were of the order of 320 ppbv (±2.8%), 1950 ppbv (±2.8%), and 180 ppbv (±2.8%), respectively. The measurement precision has been deduced from the reproducibility of the in-flight calibrations, which is ±3.5% for CO and N_2O at the 1σ level. This is in good agreement with the in-flight scatter of the 5 s averaged data, which is of the order of ±10 ppbv (3σ) for N_2O and ±8 ppbv (3σ) for CO, respectively. Methane measurements suffered from a strong optical interference (etalon effect), which resulted in a drift of the instrument background with an amplitude of several 100 ppbv. This resulted in a severe degradation of the precision of CH_4 measurements (>10%). Therefore the CH_4 measurements will not be considered in this study.

[9] A nondispersive infrared monitor was used to measure CO_2 at 1 Hz resolution. The instrument is based on a commercial LI-COR type 6262 instrument, which is operated in a differential mode. For airborne operation the instrument has been stabilized against temperature variations, while the incoming air was pressurized to 1050 hPa using a Teflon diaphragm pump. Ambient air is measured relative to a calibration gas standard in the reference cell, which is held at the same pressure and temperature as the measurement cell. The standard and a span gas are added regularly upstream of the pump for in-flight calibration of the instrument. Calibration and span gases are taken from tanks, which are analyzed before and after the campaign relative to a primary standard. The overall uncertainty of the CO_2 concentration measurement at 1 s time resolution is ±0.8 ppmv. Because of an instrument malfunction, no CO_2 data are available for flight STR-7.

[10] A modified pressure-independent chemiluminescence monitor (Bendix 8002) based on the reaction with ethylene was used to measure ozone at 1 Hz time resolution with a precision of 2% [*Bregman et al.*, 1995]. During the field phase the ozone monitor has been checked with an external ozone generator. The absolute calibration is based on titration with a NO standard gas, which is performed before and after the campaign. The accuracy of the measurements is about 5%. Because of an operator error, no ozone data were obtained during flight STR-5.

[11] A semiautomated grab sampling system capable of filling nine stainless steel canisters (2.5 L) per flight, pressurized to approximately 2.5 bar, was employed on the Citation for postflight NMHC analysis [*Lelieveld et al.*, 1999]. The air is sampled from a backward facing 1/2 foot stainless steel inlet. A MB-602 metal bellows pump is used to consecutively evacuate, flush (5 min), and fill a canister, which takes up to 3 min at the highest flight levels. The sequence for the collection of an air sample is started by a manually operated switch controlled by the flight operator in the cabin. Prior to the campaign the canisters were cleaned (heated and flushed), filled with clean nitrogen, and blank tested. Within a week after collection the air samples were sent to the Centre for Atmospheric Chemistry at York University for analysis by gas chromatography. The air sample analysis at York University was performed on a HP 5890 gas chromatograph equipped with flame ionization detection (FID) for nonmethane hydrocarbons and electron capture detection (ECD) for halocarbons. The analysis starts by preconcentrating 1 to 2 L of sample air onto a liquid Argon cooled trap (15 cm of 1/8 inch stainless tubing filled with glass beds). The amount of sample air is determined by a chosen vacuum reference volume behind the trap. By heating and flushing the trap with carrier gas the preconcentrated compounds are removed to be further concentrated on a fused silica loop with liquid nitrogen (''cold spot'') which is located directly before the column. Finally, the ''cold spot'' is rapidly heated and flushed to release the hydrocarbons onto the capillary column (J&W GS-Gaspro; 0.32 mm ID, 60 m long) for separation and detection by ECD and FID. Calibration is performed on a routine basis with commercial standard mixtures with an accuracy better than 5%. The precision lies between 2 and 5% depending on the species for concentrations larger than 10 pptv. The following hydrocarbons have been analyzed: ethane, ethyne (acetylene), propane, *n*-butane, methylpropane (isobutane), 2-methyl-1,3-butadiene (isoprene), *n*-pentane, 2-methylbutane, 2,2-dimethylpropane, benzene, cyclohexane, methyl-cyclopentane, *n*-hexane, 2-methyl-pentane, 3-methylpentane, 2,2-dimethylbutane, 2,3-dimethylbutane, toluene, methylcyclohexane, *n*-heptane, ethyl-benzene, *o*-xylene, *p*, *m*-xylene, *n*-octane, *n*-nonane, and methyl chloride. A selection of these gases is used in the present discussion.

4. Air Mass Classification

[12] Air mass origins (Table 1) have been deduced from 10 day backward trajectories based on three-dimensional (3-D) wind field analyses from the European Centre for Medium Range Weather Forecasts (ECMWF), using the KNMI trajectory model [*Scheele et al.*, 1996]. Trajectories have been calculated at 1 min intervals along the flight tracks. Following *Shipham et al.* [1994], we classified air masses as polar, midlatitudinal, or (sub)tropical according to their geographical location 96–144 hours prior to the flight. Air masses originating from latitudes higher than 50°N were classified as polar, and those with an origin south of 30°N were classified as (sub)tropical. Air masses originating between 30° and 50° were classified as midlatitudinal. Based on the 1 min resolution of the trajectories, 39% of the air masses in the upper troposphere were classified as (sub)tropical, 49% wer classified as midlatitudinal, and 12% were classified as polar.

[13] Figure 2 shows the 10 day backward trajectories for three individual flights. Figure 2a shows back trajectories for STR-2. For this flight the majority of the trajectories indicate an air mass origin north of 50°N. Parts of flights STR-1, 2, 4, 5, and 8 pertain to this category. An air mass of midlatitudinal origin, traveling over the southwestern part of the United States, was inferred for the majority of trajectories calculated for STR-6 (Figure 2b). Similar air mass trajectories were observed for parts of STR-1, 3,

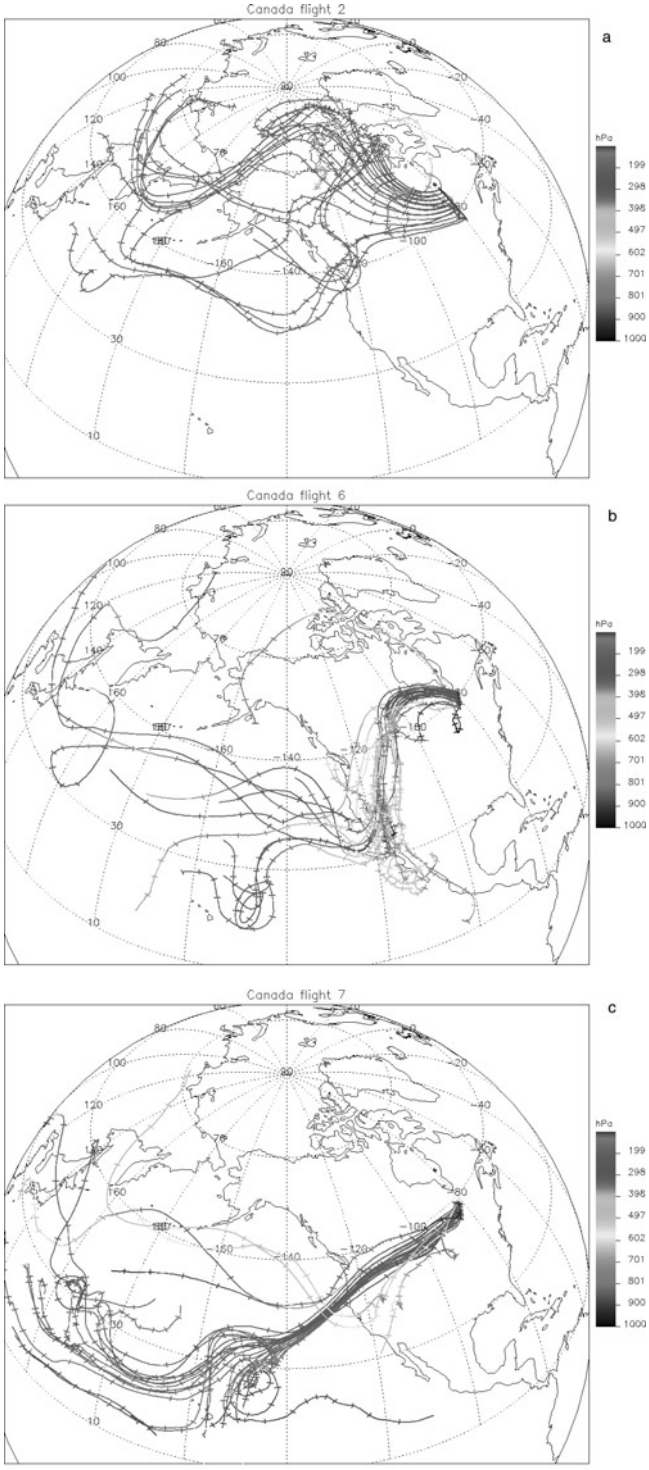

Figure 2. Ten day back trajectories for (a) a polar (STR-2), (b) a midlatitudinal (STR-6), and (c) a (sub)tropical (STR-7) air mass origin. Ticks indicate 12 hour intervals, while the color code indicates the pressure in hectopascals. See color version of this figure at back of this issue.

4, 7, and 8. (Sub)tropical air masses were encountered exclusively during parts of STR-7 (Figure 2c; see also case study) and STR-3. Mean vertical profiles of tropospheric O_3, CO, and CO_2 concentrations for the three air mass categories are presented in Figure 3. Mean, median, and the central 67% concentration values (i.e., the 16.5% and 83.5% percentiles) were calculated from 5 s averages of high-temporal-resolution data, which have been binned into 500 m altitude intervals. Stratospheric measurements were excluded by applying two selection criteria: (1) $O_3 <$ 120 ppbv and (2) ECMWF potential vorticity (PV) < 2.5 potential vorticity units (PVU) = 10^{-6} K m^2 kg^{-1} s^{-1}). Note that data below approximately 8 km, corresponding to the lowest constant altitude flight level, were obtained exclusively in the vicinity of Timmins during takeoff and landing.

[14] The Arctic profiles (Figure 3a) are composed of data from flights STR-1, 2, 4, 5, and 8. No O_3 was measured on STR-5. Except for STR-2 all flights contribute to the midlatitudinal profiles (Figure 3b), with a dominant input from STR-6. Air masses of (sub)tropical origin were only sampled in the upper troposphere. The corresponding profiles are shown in Figure 3c.

[15] The Arctic background conditions are characterized by steadily increasing O_3 concentrations with altitude in the troposphere, from approximately 20 ppbv above the boundary layer (1500 m) to values around 60 ppbv at the tropopause (10.5 km) (see Figure 3a). The CO concentration, on the other hand, is rather constant over the entire troposphere, varying between 113 and 145 ppbv (Figure 3b). Closer inspection of Figure 3a reveals a fine structure in the observed free tropospheric O_3 gradient, with a layer of nearly constant O_3 mixing ratios of the order of 44 ppbv between 4250 and 7250 m. Because of the much higher variability, a similar layering is not observed in the free tropospheric CO profile. The CO_2 profile shows a rapid increase from the surface to 3 km altitude, followed by a slower increase up to the tropopause. The gradual increase above 3 km is relatively small compared to the high variability in each layer. Compared to earlier findings during the ABLE 3B campaign, average CO levels for Arctic background conditions during STREAM 1998 are relatively high (STREAM, 122–138 ppbv; ABLE 3B, 96–98 ppbv) [*Harriss et al.*, 1994b], while O_3 mixing ratios are comparable for the two campaigns, being 45 to 60 ppbv [*Shipham et al.*, 1994; *Browell et al.*, 1994]. Average upper tropospheric (between 7 km altitude and 1 km below the local tropopause) CO concentrations of 120.7 ± 36.6 ppbv have been observed over Fairbanks, Alaska, in July 1997 by *Herman et al.* [1999], in agreement with our findings. The back trajectories (e.g., Figure 2a) indicate that air masses of this category typically traveled from northeastern Asia across the Arctic. It is quite conceivable that continental sources, including biomass burning, have added CO to these air masses.

[16] Lower CO concentrations of the order of 95–115 ppbv between 2 and 10 km altitude and a much lower variability have been observed in air masses of midlatitudinal origin (see Figure 3b). Ozone concentrations in this category are very similar to the Arctic profile except for the layers below 3 km, where O_3 exceeds the values in polar air by 5 to 10 ppbv. Above 10 km altitude the stratospheric influence is clearly noticeable in the midlatitudinal profile with increasing O_3 and decreasing CO. Mean CO_2 concentrations are higher than in the Arctic profile throughout the troposphere, in particular below 6 km altitude, but the tendency to increasing concentrations with increasing altitude is smaller. Only the layers above 10 km show significantly higher concentrations as compared to the layers below.

[17] The (sub)tropical profiles (Figure 3c) are composed of measurements of flights STR-3 and STR-7. The results of the two flights are presented separately, because they represent chemically distinct air masses. Air masses sampled during STR-3 were strongly affected by recent convective activity upwind of the flight track [*Lange et al.*, 2001]. Despite their tropical origin derived from back trajectories, these samples therefore have a pronounced midlatitudinal signature. The measurements of STR-7, on the other hand, were not affected by recent convection and show very low

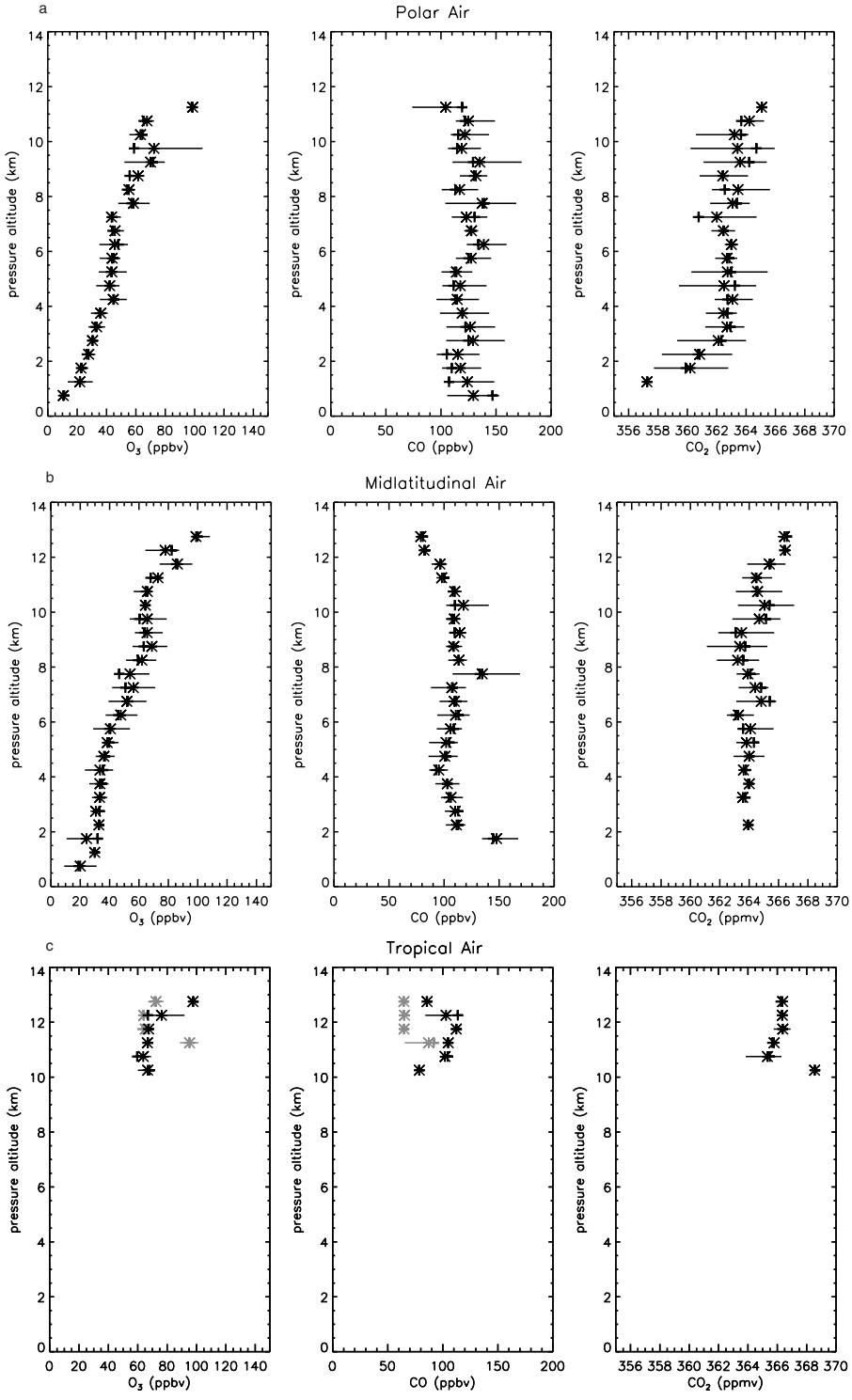

Figure 3. Median (vertical lines), mean (stars), and central 67% concentrations values for ozone, CO, and CO_2 profiles averaged over 500 m bins for (a) a polar air mass origin, (b) a midlatitudinal air mass origin, and (c) a (sub)tropical air mass origin. Data in Figure 3c presented in black were obtained during STR-3, while data in gray were obtained during STR-7.

CO concentrations of the order of 60 to 70 ppbv between 11 and 13 km. Although these CO mixing ratios are typical for those found in the lowermost stratosphere (not shown), the low O_3 mixing ratios of only 65 to 70 ppbv indicate that these air masses are not of stratospheric origin. Instead, the air probably had an origin in the upper troposphere over the tropical Pacific, as indicated by the back trajectories in Figure 2c. Similarly low CO mixing ratios (69.9 ± 6.9 ppbv) have been observed over central and eastern Canada during the ABLE 3B expedition in July–August 1990 during episodes of very long range transport of air from the tropical Pacific Ocean. Tropical and subtropical free tropospheric CO concentrations over the Pacific in the summertime

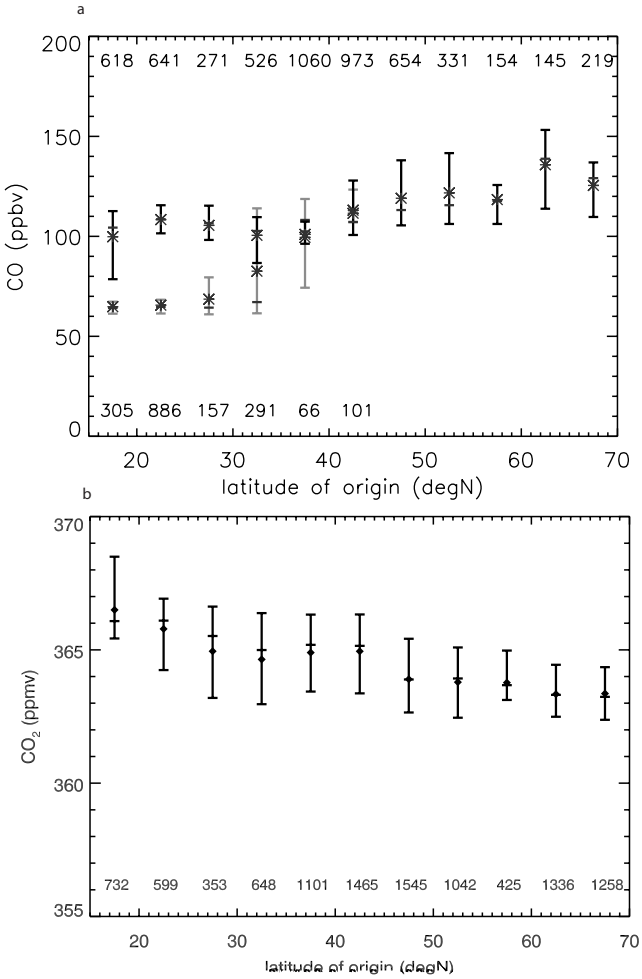

Figure 4. Latitudinal cross section of upper tropospheric (a) CO and (b) CO_2 concentrations. The data have been binned according to the air mass origin deduced from 5 day back trajectories. Median and mean values are indicated by horizontal lines and stars, respectively. Vertical lines indicate the central 67% of the data. Gray data points in Figure 4a represent observations obtained exclusively during STR-7. The numbers indicate the number of data points in each bin.

have been reported from a number of studies. *Herman et al.* [1999] mention upper tropospheric CO mixing ratios of 73.2 ± 14.6 over NASA Ames, California (37°N), and 65.8 ± 7.3 over Barbers Point, Hawaii (21°N). For Pacific Exploratory Mission (PEM)-Tropics (August–September 1996), *Gregory et al.* [1999] report median CO mixing ratios over the tropical Pacific north of the Intertropical Convergence Zone (ITCZ) between 8 and 10 km of the order of 58 ppbv and O_3 mixing ratios of the order of 35 ppbv. The comparison with these summertime CO values in the upper troposphere south of 30°N supports our trajectory-based interpretation of a tropical air mass origin encountered during STR-7 over Canada. However, it should be emphasized that the observed O_3 mixing ratio during STREAM is much higher than indicated by observations over the tropical Pacific made during PEM-Tropics. This could be due to the higher-altitude origin (approximately 15 km) deduced from the back trajectories for the STREAM measurements. As discussed by *Folkins et al.* [1999], O_3 mixing ratios in the inner tropics start increasing toward stratospheric values near 14 km.

[18] While the expected strong anticorrelation between CO and O_3 was observed in the lowermost stratosphere (not shown), no significant relation among these species was found in the free troposphere [*Hoor et al.*, 2002]. This contrasts with ground-based studies in the continental boundary layer, where a significant positive correlation has been frequently observed, with a $\Delta O_3/\Delta CO$ value of the order of 0.3, indicating photochemical ozone production in polluted air masses [*Chin et al.*, 1994; *Parrish et al.*, 1998]. During the STREAM 1998 mission, significant increases of the O_3 concentration have been observed in the upper troposphere, in particular above 6–7 km altitude (Figures 3a and 3b). Upper tropospheric O_3 enhancements are due to either in situ photochemical production or downward mixing of ozone-rich air from the stratosphere. To estimate the influence of stratosphere troposphere exchange (STE) events on the ozone budget of the upper troposphere, the potential vorticity history of the air masses was analyzed. Trajectories that stayed in the stratosphere for 3 consecutive days before entering the troposphere in the last 6 hours were taken as indicative of STE events. Thus 11% of the upper tropospheric O_3 measurements between 8 km and the local tropopause were found to be influenced by cross-tropopause transport of O_3-rich air from the stratosphere.

[19] The observed low-O_3 concentrations in the lower troposphere are most probably due to dry deposition at the surface, the reduced chemical lifetime of O_3 against oxidation by the reaction of $O(^1D) + H_2O$ after O_3 photodissociation, and titration with NO in the vicinity of the airport. Note that the O_3 profile of Arctic origin (Figure 3a) indicates near-zero concentrations near the surface. These air masses have traveled mostly over land, where O_3 deposition velocities are relatively high. The close contact with the surface is also reflected in reduced CO_2 levels (Figure 3a), which can be explained by significant uptake of CO_2 by vegetation during daytime. CO, which is not influenced by dry deposition, shows increasing concentrations near the surface (Figure 3a). Wildfires in the Canadian boreal forests are likely to be significant contributors to these elevated CO values.

[20] In general, measured CO and CO_2 are anticorrelated throughout the troposphere, while in the lower stratosphere the correlation is positive. The CO_2 profile exhibits an "inverted C-shape," with low values in the lower troposphere and stratosphere and highest mixing ratios in the upper troposphere. This finding is consistent with earlier observations in high and middle latitudes in summer [*Huntrieser et al.*, 1998; *Nakazawa et al.*, 1991] and a model simulation of the CO_2 seasonal cycle in the upper troposphere and lower stratosphere by *Strahan et al.* [1998]. The significant decrease of CO_2 with decreasing altitude (in particular below 3 km) is due to uptake by the vegetation.

[21] Figures 3a–3c suggest a pronounced dependence of the concentrations of CO and CO_2 on air mass origin. This is demonstrated more clearly in Figures 4a and 4b, where CO and CO_2 concentrations in the upper troposphere (between 8 km and the local tropopause) are binned with respect to the latitude of the air mass origin deduced from the 5 day back trajectories. While CO

Table 2. Mean (1σ Standard Deviation) CO, CO_2, and NMHC Concentrations for the Different Air Mass Regimes

	Polar	Midlatitudes	Tropics[a] (STR-3)	Tropics (STR-7)
Altitude, km	9.7–10	7.6–13.1	10.5–12	11–13
O_3, ppbv	61 (4)	66 (14)	66 (7)	70 (6)
CO_2, ppmv	362.3 (1.8)	364.4 (1.5)	366.2 (1.4)	–
CO, ppbv	121 (11)	107 (25)	104 (14)	64 (2)
C_2H_2, pptv	115 (46)	119 (43)	106 (15)	39 (14)
C_2H_6, pptv	1149 (70)	983 (385)	1283 (427)	424 (86)
C_3H_8, pptv	178 (0)	207 (102)	386 (224)	20 (5)
n-C_4H_{10}, pptv	12 (9)	35 (25)	56 (39)	4 (1)
i-C_4H_{10}, pptv	15 (5)	21 (11)	33 (17)	4 (4)
Benzene, pptv	25 (6)	38 (33)	31 (10)	6 (3)
Toluene, pptv	8 (7)	8 (13)	5 (2)	2 (1)
CH_3Cl, pptv	539 (2)	578 (36)	591 (16)	611 (11)

[a] With recent convective input of midlatitude air.

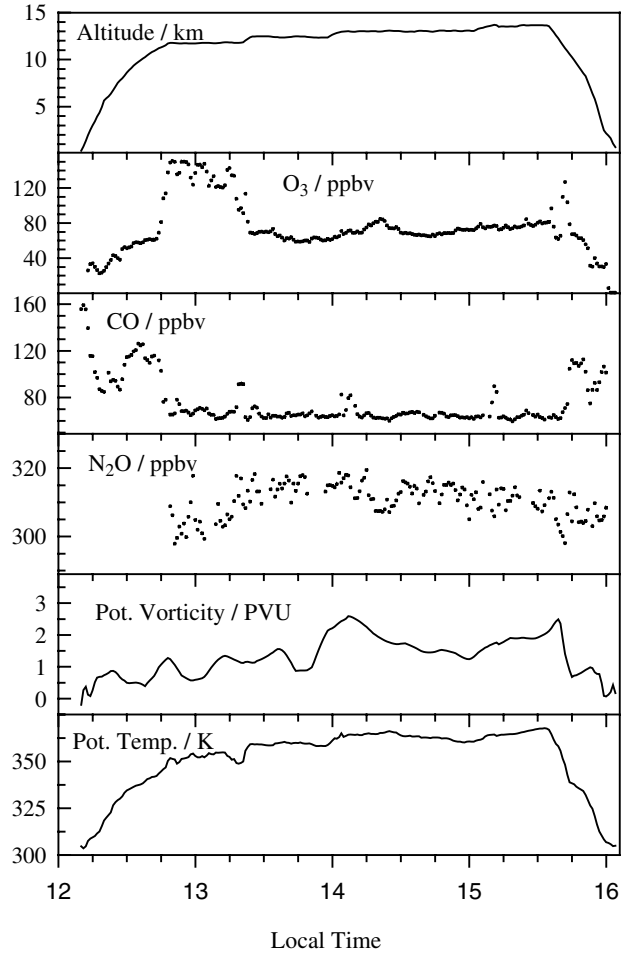

Figure 5. Time series of pressure altitude, O_3, CO, N_2O, analyzed potential vorticity, and potential temperature for STR-7 performed ahead of the approaching cold front.

concentrations increase with increasing latitude, reflecting the latitudinal distribution of pollution sources in the Northern Hemisphere and the stronger tropical/subtropical sink due to increasing OH concentrations at low latitudes, CO_2 exhibits a significant concentration decrease with latitude. This is in qualitative agreement with the model study by *Strahan et al.* [1998], which indicated a strong latitudinal gradient of the tropospheric CO_2 concentration in summer, with highest values in the tropics and lowest values in the Arctic.

[22] In recent years a number of studies have been published that use measurements of NMHC to infer chemical signatures of tropospheric air masses [*Smyth et al.*, 1996, 1999; *Talbot et al.*, 1996; *Gregory et al.*, 1996, 1999]. In particular, measurements of relatively long-lived hydrocarbons (e.g., alkanes) can be used to complement an air mass classification based on back trajectory calculations [*Smyth et al.*, 1996, 1999]. Here we use a selection of NMHC (Table 2) with chemical lifetimes ranging from 3 to 4 days for toluene up to three months for ethane, which have predominantly biomass-burning and anthropogenic sources (combustion, gasoline evaporation, industrial processes) [*Warneck*, 1988]. We also use CH_3Cl (lifetime ~1.5 years), which has both oceanic and biomass-burning sources [*Graedel and Keene*, 1995]. Average values for the concentration of ethane, acetylene, propane, *n*-butane, *i*-butane, benzene, toluene, and CH_3Cl for the various air mass regimes are listed in Table 2. To calculate average mixing ratios for Arctic air masses, samples from STREAM flights STR-1, STR-4, and STR-8 have been averaged (six samples). Values for air masses of midlatitudinal origin are deduced from 18 samples taken during STR-1, 3, 6, and 8, while average concentrations for (sub)tropical air masses were evaluated separately for STR-3 (seven samples) and STR-7 (six samples). Because of the limited number of samples the statistics for these calculations is poor. Therefore we will use the NMHC data in a more qualitative way to support our air mass classification, which is mainly based on back trajectories. In addition, average CO and CO_2 values were calculated for the periods of NMHC sampling. These values are also listed in Table 2.

[23] Nonmethane hydrocarbons which are predominantly produced by combustion processes (acetylene, benzene, toluene) have highest concentrations in air masses of midlatitudinal origin. The highest concentrations of ethane, propane, *n*-butane, and *i*-butane are measured in these air masses, which is consistent with presumed anthropogenic sources. The lowest tropospheric concentrations for these species are found in air masses of tropical origin, in particular those encountered during STR-7, while CH_3Cl concentrations are highest. This is consistent with a general trend of increasing CH_3Cl concentrations with decreasing latitude, caused by the large maritime and biomass-burning sources of this species in the tropics [*Graedel and Keene*, 1995]. A comparison with NMHC measurements during PEM-Tropics (August to October 1996) obtained over the tropical Pacific (median position 13.1°N, 156.2°W) at 8 to 10 km altitude shows good agreement (ethane, 430 pptv/424 pptv (PEM-Tropics/STR-7); acetylene, 30 pptv/39

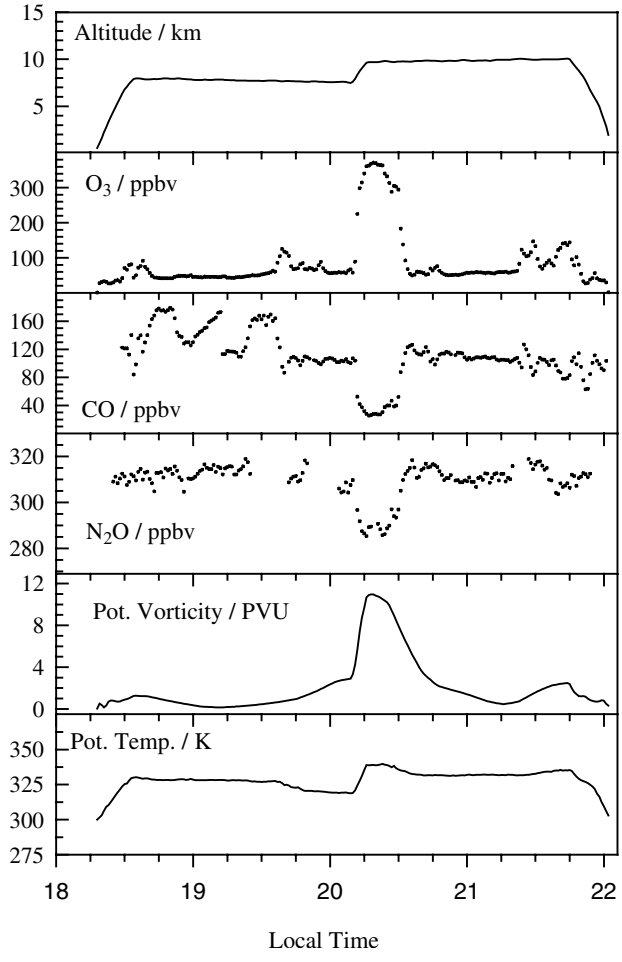

Figure 6. Time series of pressure altitude, O_3, CO, N_2O, analyzed potential vorticity, and potential temperature for STR-8 performed behind the cold front.

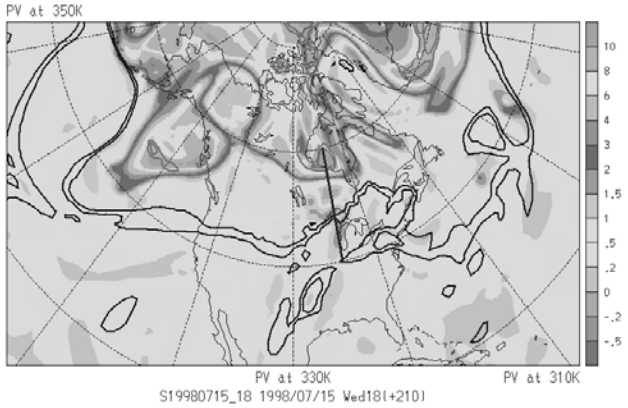

Figure 7. Analysis of the potential vorticity at the 330 K level for 15 July, 1800 UTC. Superimposed are the PV = 2 and PV = 3 lines at 350 K (black lines) and 310 K (green lines). The black lines mark the position of the subtropical jet at 350 K, while the colored contours at 2–3 PVU indicate the position of the polar jet at 330 K. The blue line is the horizontal projection of the vertical cross section shown in Figure 8. See color version of this figure at back of this issue.

pptv; propane, 34 pptv/20 pptv; CH_3Cl, 562 pptv/611 pptv) [*Gregory et al.*, 1999]. The fact that NMHC concentrations observed over Canada are similar to concentrations in the anticipated source region further supports the back-trajectory-based interpretation that the transport from the tropics to high northern latitudes took place within a few days. Mean concentrations of CO and NMHC during STR-3, for which the back trajectories also indicate an air mass origin south of 30°N, are significantly higher than during STR-7 and of the same order of magnitude as observations from midlatitudes. This is due to deep convection which these air masses experienced over the central United States. For a detailed discussion of this particular flight, see *Lange et al.* [2001].

[24] Upper tropospheric NMHC concentrations in polar and midlatitudinal air masses were enhanced compared to earlier observations in the lower free troposphere during ABLE 3A in the summer of 1988 [*Blake et al.*, 1992] and during ABLE 3B in summer 1990 [*Wofsy et al.*, 1994]. The upper tropospheric NMHC concentrations during STREAM 1998 clearly represent enhanced conditions compared to background conditions in the middle troposphere as found during these earlier campaigns by other groups. Potential sources for the pollution are wildfires in the boreal forests of northern Canada, Alaska, and Siberia or anthropogenic pollution from the Great Lakes area. The ratio of C_2H_2/CO, which can be interpreted as a marker for the chemical processing of air masses [*Smyth et al.*, 1996, 1999], is of the order of 1 pptv/ppbv, which points to an "age" of these gases of the order of 5 to 7 days [*Gregory et al.*, 1999]. This is consistent with the back trajectories, which indicate that transport in the upper troposphere occurred predominately at constant altitudes and that large-scale lifting or convection from the boundary layer did not occur at least 5 days prior to the flights (Figure 2), with the exception of STR-3, which was strongly influenced by recent convection.

5. Chemical Air Mass Differences Near Fronts

[25] During the STREAM 1998 summer campaign, air masses of very different origin were often found in remarkably close proximity to each other. In particular in the vicinity of fronts and jet streams the chemical characteristics of air masses often changed within tens of kilometers. Transport of coherent air masses in the vicinity of fronts has been studied extensively over the last decades [see, e.g., *Carlson*, 1980; *Browning and Roberts*, 1994; *Wernli and Davies*, 1997; *Wernli*, 1997]; however, studies on chemical air mass differences near fronts are sparse [*Bethan et al.*, 1998; *Stohl and Trickl*, 1999]. In this section we will discuss the flights STR-7 (Figure 5) and STR-8 (Figure 6) in more detail, to demonstrate the occurrence of strong trace gas gradients close to fronts, which separate large-scale flow regimes that are chemically coherent.

[26] From 14 July to 16 July a major southward excursion of stratospheric air from high latitudes occurred over northeastern Canada. By 15 July, 1800 UTC, the intrusion had developed into a deep trough over the western part of the Hudson Bay north of Timmins (Figure 7). At the same time, the subtropical jet stream (represented by the black PV contours on the 350 K isentropic surface) advected air from the tropical/subtropical Pacific toward the region south of Timmins as can be seen from the back trajectories of this flight in Figure 2c. As a result of these particular flow conditions the polar jet stream marking the southern flank of the trough and the subtropical jet stream converged just east of Timmins in the late afternoon of 15 July. A vertical north to south cross section at 84°W to the west of Timmins (along the blue line in Figure 7) shows the two jets which were still separated at this position (Figure 8). Two tropopause breaks are evident, one near 49°N from 14 km (142 hPa) to 10 km (265 hPa) and a second one near 54°N from 10 km (265 hPa) to 6 km (472 hPa) altitude. Both are associated with a jet with a maximum wind speed of 40 to 45 ms^{-1}. The potential temperature contours further indicate the presence of a cold front associated with the upper level trough at the latitude of Timmins. Also shown in Figure 8 is the projection of the two flights performed on this day onto the vertical north-south cross section.

[27] The first flight (STR-7, 1600–2000 UTC; local time is UTC-4 hours) was carried out ahead of the cold front in a southwestward direction parallel to the cloud band associated with the approaching cold front. The second flight (STR-8, 2200–0200 UTC) was flown mainly behind the front toward the center of the upper level trough over the western Hudson Bay. Time series for the individual flights are shown in Figures 5 and 6, respectively. The flight tracks are shown in Figure 9 together with the frontal clouds as seen by GOES 8. Also shown are the maximum ascending and descending airflows associated with the depression

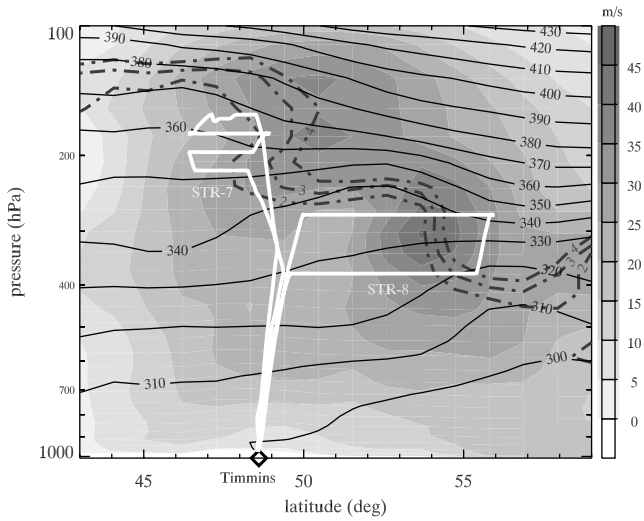

Figure 8. Vertical cross section of wind speed, potential temperature (solid lines), and potential vorticity (dashed lines at 2, 3, and 4 PVU, respectively) for 15 July 1998. The cross section is taken along the blue line in Figure 7. The flight tracks of flight STR-7 and 8 are superimposed on the figure.

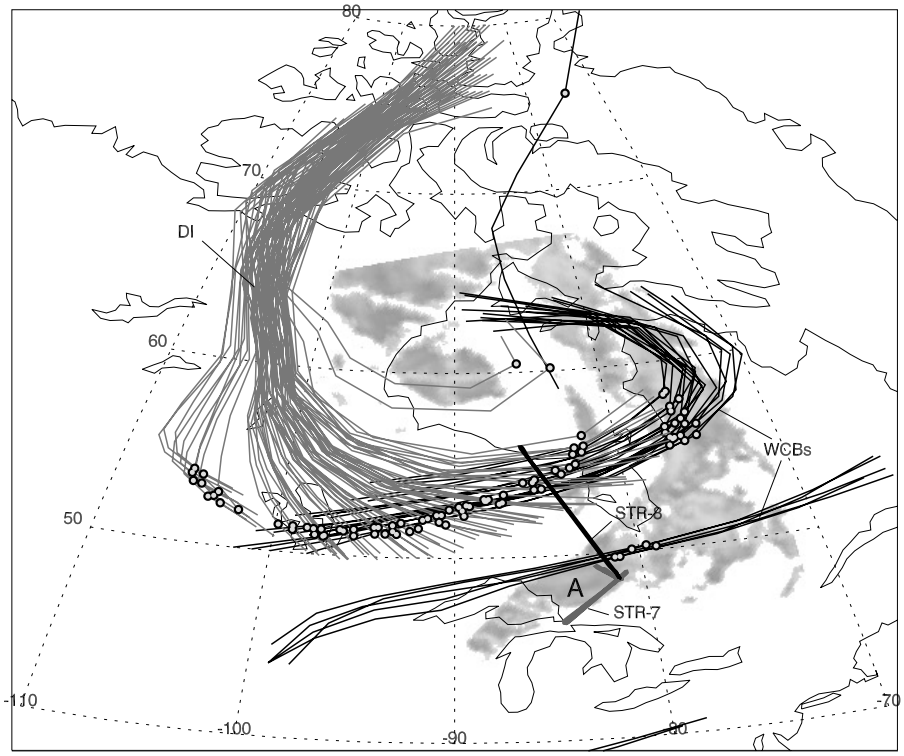

Figure 9. Flight tracks of STR-7 (thick grey line) and STR-8 (thick black line) plotted over the frontal cloud band as seen in the GOES 8 IR satellite image at 1745 UTC on 15 July. Superimposed are trajectories corresponding to coherent airflows showing either a strong ascent (thin black lines, $\Delta p < -400$ hPa) or descent (thin grey lines, $\Delta p > 300$ hPa) between 14 and 16 July. Circles on the trajectories mark the position of each air parcel at 1800 UTC on 15 July, roughly corresponding to the central time of STR-7. WCB, warm conveyor belt.

over the Hudson Bay. Using the trajectory tool "Lagranto" [*Wernli and Davies*, 1997], (1) 2 day forward trajectories were calculated from a regular mesh over the Northern Hemisphere and (2) selection criteria were applied to select air parcels with either a strong ascent ($\Delta p < -400$ hPa) or a strong descent ($\Delta p > 300$ hPa). The airflows detected in this way represent major downward intrusions of dry air from polar regions (Figure 9, thin grey lines) and two moist ascending airflows in the region of the cold front (thin black lines). The two separate ascending airflows are associated with a distinct substructure of the front: Maps of temperature and humidity at 850 hPa (not shown) reveal that while there was only a single temperature front, there were two distinct steps in humidity. In the very moist air near the southern humidity front, strong convective activity developed (labeled "A" in Figure 9) below the axis of the subtropical jet. Low-level convergence of air into this region resulted in large-scale ascent as traced by the southern bundle of ascending trajectories. The northern cluster is more typical of a warm conveyor belt (WCB), in which warm and moist air rises ahead of the approaching cold front.

[28] In Figure 10 the trace gas concentrations of O_3 (Figure 10a) and CO (Figure 10b) are shown as a function of altitude and latitude (both flights were roughly oriented in a north-south direction). Measurements south of 48.5°N were obtained during STR-7 in the warm sector ahead of the approaching front (see also Figure 3c for measurements obtained during this flight), while further north we flew behind the front in the cold sector (STR-8).

[29] Backward trajectories for both flights show that the origins of these prefrontal and postfrontal air masses were very different. As indicated in section 4, air masses ahead of the cold front (STR-7) originated predominately from the tropical Pacific Ocean (Figure 2c), while those behind the front were of midlatitudinal to Arctic origin. STR-7 mainly consisted of four stacked flight levels between 11.5 (216 hPa) and 13.1 km (160 hPa). CO mixing ratios on these four levels show only little variability at very low concentrations of the order of 60–70 ppbv (Figure 10b). Surprisingly, enhanced O_3 in excess of 120 ppbv indicative of stratospheric air was observed at the lowest flight leg (11.5 km, 216 hPa), while the ozone concentrations at the higher flight levels decrease to values of about 60 ppbv, indicative of a strong tropospheric influence. This interpretation is further supported by measurements of N_2O and NO_y. On the lowest flight level the average N_2O mixing ratio was 309.6 ± 2.2 ppbv, while NO_y was of the order of 1.8 ± 0.4 ppbv, values typical for the lowermost stratosphere, directly above the tropopause. At the higher flight levels, N_2O was somewhat enhanced (312.8 ± 4.8 ppbv), while NO_y levels were significantly lower (0.99 ± 0.15 ppbv). Differences with respect to NMHC levels in both air masses were small, though consistent with the above interpretation. Mixing ratios for a number of long-lived hydrocarbons for the upper three flight levels are listed in Table 2 (labeled "Tropics (STR-7)"), while the concentrations levels measured on the lowest flight level of STR-7 were similar to those obtained for the Arctic stratospheric background.

[30] The backward trajectories shown in Figure 2c support this picture of a layer of stratospheric air below tropospheric air: Air parcels observed at the two highest flight levels (12.5 (177 hPa) and 13.1 km (160 hPa)) were advected from the upper troposphere over the tropical Pacific Ocean during the previous 10 days. They steadily descended from initial altitudes of 120 to 100 hPa to the flight levels of about 190 hPa. Some of the trajectories even appear to originate from the Intertropical Convergence Zone (ITCZ) located between 5°N and 10°N as derived from satellite images. The back trajectories for the lowest level largely originate from higher latitudes and crossed the tropopause from the stratosphere to

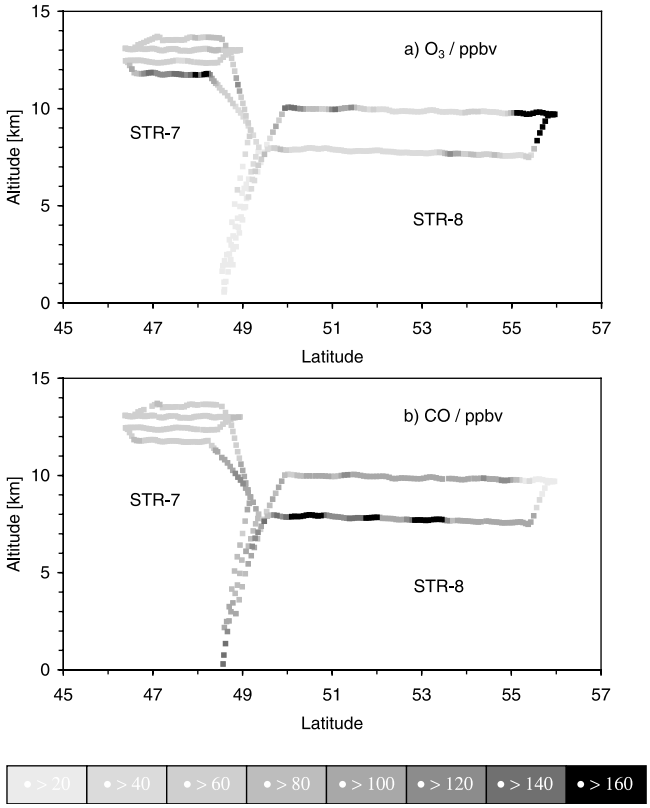

Figure 10. Latitude-altitude plot of the (a) O_3 and (b) CO concentrations during STR-7 and STR-8, ahead and behind a surface cold front. The data points colored in brown indicate mixing ratios in excess of 160 ppbv for O_3 and CO, respectively. See color version of this figure at back of this issue.

the troposphere in agreement with the chemical signatures of this air mass. Potential vorticity values evaluated along the trajectories decreased from stratospheric values of about 4 PVU four days earlier to tropospheric values of 1.5 PVU at the time of the measurement.

[31] During the ascent to the first constant flight level a strong layering, especially in CO, was observed (see Figure 10). Between 4 and 8 km a layer with CO concentrations on the order of 80–90 ppbv was sampled, a concentration level significantly lower than typical values observed during the campaign (compare Figure 3b). Directly above and below this layer the CO concentrations are significantly higher (110–120 ppbv), levels more typical for continental midlatitude conditions.

[32] Back trajectories indicate that the air masses observed between 4 and 11 km followed a similar path as the southern bundle of ascending trajectories shown in Figure 9. They were advected from the Pacific Ocean within 4 to 6 days and experienced a pronounced ascent during the last 24 to 48 hours ahead of the approaching cold front. However, while the air masses between 4 and 8 km always remained above 3 km altitude during the passage from the Pacific, the air between 8 and 9 km possibly originated from the polluted boundary layer, as the trajectories indicate a recent ascent from only 2 km above the surface. The low CO values at intermediate levels (4–8 km altitude) can thus be interpreted as free tropospheric midlatitude background concentrations typically observed over the Pacific Ocean. In contrast, the enhanced CO levels at 8 to 11 km can most likely be attributed to large-scale ascent or local convective transport from the boundary layer, or both. The GOES IR satellite image of the clouds, obtained at 1745 UTC, suggests that in particular the ascent to the first constant flight level was influenced by convective activity (region A in Figure 9).

[33] Behind the surface cold front, significantly higher concentrations of CO and NMHC were observed during STR-8 (north of 49° in Figure 10). Between 49° and 53°N on the lowest flight level (approximately 8 km), CO concentrations in excess of 160 ppbv and enhanced NMHC concentrations (e.g., C_2H_2 = 238 pptv, C_2H_6 = 2.25 ppbv, and C_3H_8 = 394 pptv) indicate strong pollution of the middle troposphere, most probably associated with emissions from a wildfire reported north of Lake Superior. At the most northerly point of the flight a deep intrusion of stratospheric air into the middle troposphere at 56°N was encountered, which could be unambiguously identified by increased O_3 concentration of more than 350 ppbv and very low CO concentrations on the order of 20 ppbv. The southward extension of this intrusion at the time of the flight is represented by the circles on the grey trajectories in Figure 9. A detailed discussion of the stratospheric intrusion will be given in a future publication (J. Beuermann et al., High-resolution measurements and simulations of stratospheric and tropospheric intrusions in the vicinity of the jet stream, submitted to *Geophysical Research Letters*, 2001). On the return leg at approximately 10 km altitude, CO levels varied from about 120 ppbv in the northern section to about 100 ppbv in the southern section. These concentrations are in good agreement with an Arctic origin at the beginning and a midlatitude origin toward the end of the flight leg as derived from the back trajectories.

[34] It has been known for decades that the stirring induced by synoptic disturbances can create narrow elongated structures termed "fronts," which are characterized by strong horizontal gradients in temperature and humidity separating air masses of different origin (for instance [*Bjerknes*, 1910]). The case study of the passage of a cold front presented here suggests that these sharp air mass transitions are also reflected by sharp gradients in the concentrations of atmospheric tracers. A salient feature of vertically deep cold fronts is the upper level jet stream. In our particular case the subtropical and polar jet converged over the area of Timmins. To the south of the subtropical jet, air of tropical origin was advected to the upper troposphere over Canada, which was related to a remarkably high and eroded tropopause. Across the two jets the air mass origin changed from tropical to Arctic. This is in qualitative agreement with the confluence of air of low- and high-latitude origin in an upper level jet described in the conceptual model of airflow relative to the movement of a cyclone by *Carlson* [1980]. Accordingly, the chemical characteristics changed from very low CO and NMHC concentrations in the tropical air mass to high values in the cold sector to the north of the polar jet.

[35] Three physically and dynamically significant airstream patterns have been identified within midlatitude cyclones, the warm and cold conveyor belts, and the dry intrusion (see reviews by *Browning* [1990] and *Carlson* [1980]). The effect of these airflows on the distribution of tracers in the upper troposphere is still not well known. Depending on the origin of air transported in a WCB, whether polluted continental or unpolluted maritime, the characteristics of WCBs are likely to range from highly polluted to very clean [*Stohl*, 2001]. As described above, indications for the presence of a WCB with a base in the polluted continental boundary layer were found at 8 to 11 km altitude during the ascent to the first flight level on STR-7. However, convective activity, which is often triggered by an approaching cold front and embedded in WCBs, is likely to have masked the chemical characteristics of this slowly ascending air mass by rapid vertical injection of polluted air from the local boundary layer.

6. Conclusions

[36] During summer 1998, eight measurement flights were performed over the subarctic wetlands of central northern and northeastern Canada, extending the 1990 ABLE 3B expedition

[*Harriss et al.*, 1994a] to the upper troposphere and lowermost stratosphere. Our classification of middle and upper tropospheric air mass origins is in good agreement with that of ABLE 3B. However, compared to ABLE 3B, significantly higher CO mixing ratios were observed in Arctic background air. *Harriss et al.* [1994b] have shown that plumes from forest fires can significantly enhance background hydrocarbon and CO mixing ratios in the lower troposphere on a regional scale. Thus the higher CO and NMHC concentrations in the upper troposphere during STREAM 1998 might indicate an even stronger influence of biomass burning on the composition of the troposphere in 1998 compared to 1990. This interpretation concurs with observed yearly increases in the fire activity in the 1990s in Canada and Siberia [*Waibel et al.*, 1999; *Kasischke et al.*, 1999]. On the other hand, high-altitude upper tropospheric pollution layers due to biomass burning were observed only during a short portion of flight STR-8 and the first transfer flight back to Europe from Timmins to Kujack on 19 July 1998 [*Lange*, 2001], indicating that the dominance of forest fire emissions as a source of CO and NMHC in the lower and middle troposphere during summer over northern Canada, as was observed during the ABLE 3B mission, cannot be extended to the upper troposphere during the July 1998 STREAM flights. Unfortunately, the NMHC data coverage is too sparse to allow a representative estimate of the contribution of different pollution sources via the determination of enhancement ratios relative to CO for selected hydrocarbons. The relatively high levels of CO and NMHC in the middle and upper troposphere over Canada, and the simultaneous observation of high NO_x concentrations due to lightning production [*Lange et al.*, 2001], provide ideal conditions for in situ photochemical O_3 production. Furthermore, long-range transport from the tropical Pacific Ocean also strongly affects the composition of the upper troposphere over the Hudson Bay lowlands by advection of cleaner, less polluted air masses toward this region. A case study of measurements performed on 15 July confirms that sharp discontinuities in trace gas levels are associated with coherent airflows in the vicinity of a cold front. Both the analysis of the trace gas measurements and the results from a trajectory model are consistent with the conveyor belt concept of synoptic disturbances. The latter give rise to steep gradients in natural (e.g., stratospheric O_3) and pollutant gases on synoptic scales.

[37] **Acknowledgments.** We gratefully acknowledge the excellent collaboration with the entire Citation team and the crew from the Technical University of Delft. The STREAM project was supported by the European Union (DG XII).

References

Bachmeier, A. S., M. C. Shipham, E. V. Browell, W. B. Grant, and J. M. Klassa, Stratospheric/tropospheric exchange affecting the northern wetlands regions of Canada during summer 1990, *J. Geophys. Res.*, *99*, 1793–1804, 1994.

Bethan, S., G. Vaughan, C. Gerbig, A. Volz-Thomas, H. Richer, and D. A. Tiddeman, Chemical airmass differences near fronts, *J. Geophys. Res.*, *103*, 13,413–13,434, 1998.

Bjerknes, V., Synoptical representation of atmospheric motions, *Q. J. R. Meteorol. Soc.*, *36*, 267–286, 1910.

Blake, D. R., D. F. Hurst, T. W. Smith Jr., W. J. Whipple, T.-Y. Chen, N. J. Blake, and F. S. Rowland, Summertime measurements of selected nonmethane hydrocarbons in the Arctic and Subarctic during the 1988 Arctic Boundary Layer Expedition (ABLE 3A), *J. Geophys. Res.*, *97*, 16,559–16,588, 1992.

Bregman, A., et al., Aircraft measurements of O_3, HNO_3, and N_2O in the winter Arctic lower stratosphere during the Stratosphere-Troposphere Experiment by Aircraft Measurements (STREAM I), *J. Geopyhs. Res.*, *100*, 11,245–11,260, 1995.

Browell, E. V., M. A. Fenn, C. F. Butler, W. B. Grant, R. C. Harriss, and M. C. Shipham, Ozone and aerosol distributions in the summertime troposphere over Canada, *J. Geophys. Res.*, *99*, 1739–1755, 1994.

Browning, K. A., Organisation of clouds and precipitation in extratropical cyclones, in *Extratropical Cyclones: The Erik Palmen Memorial Volume*, edited by C. Newton and E. O. Holopainen, pp. 129–154, Am. Meteorol. Soc., Boston, Mass., 1990.

Browning, K. A., and N. M. Roberts, Structure of a frontal cyclone, *Q. J. R. Meteorol. Soc.*, *120*, 1535–1557, 1994.

Bujok, O., et al., GHOST: A novel airborne gas chromatograph for in situ measurements of long-lived tracers in the lower stratosphere, *J. Atmos. Chem.*, *39*, 37–64, 2001.

Carlson, T. B., Airflow through midlatitude cyclones and the comma cloud pattern, *Mon. Weather Rev.*, *108*, 1498–1509, 1980.

Chin, M., D. J. Jacob, J. M. Munger, D. D. Parrish, and B. G. Doddridge, Relationship of ozone and carbon monoxide over North America, *J. Geophys. Res.*, *99*, 14,565–14,573, 1994.

Fischer, H., et al., Observations of high concentrations of total reactive nitrogen (NO_y) and nitric acid (HNO_3) in the lower Arctic stratosphere during the STREAM II campaign in February 1995, *J. Geophys. Res.*, *102*, 23,559–23,571, 1997.

Folkins, I., M. Loewenstein, J. Podolske, S. J. Oltmans, and M. Proffitt, A barrier to vertical mixing at 14 km in the tropics: Evidence from ozonesondes and aircraft measurements, *J. Geophys. Res.*, *104*, 22,095–22,102, 1999.

Graedel, T. E., and W. C. Keene, Tropospheric budget of reactive chlorine, *Global Biogeochem. Cycles*, *9*, 47–77, 1995.

Gregory, G. L., A. S. Bachmeier, D. R. Blake, B. G. Heikes, D. C. Thornton, A. R. Bandy, J. D. Bradshaw, and Y. Kondo, Chemical signatures of aged Pacific marine air: Mixed layer and free troposphere as measured during PEM-West A, *J. Geophys. Res.*, *101*, 1727–1742, 1996.

Gregory, G. L., et al., Chemical characteristics of Pacific tropospheric air in the region of the Intertropical Convergence Zone and South Pacific Convergence Zone, *J. Geophys. Res.*, *104*, 5677–5696, 1999.

Harriss, R. C., S. C. Wofsy, J. M. Hoell Jr., R. J. Bendura, J. W. Drewry, R. J. McNeal, D. Pierce, V. Rabine, and R. J. Snell, The Arctic Boundary Layer Expedition (ABLE-3B): July–August 1990, *J. Geophys. Res.*, *99*, 1635–1643, 1994a.

Harriss, R. C., G. W. Sachse, J. E. Collins Jr., L. Wade, K. B. Bartlett, R. W. Talbot, E. V. Browell, L. A. Barrie, G. F. Hill, and L. G. Burney, Carbon monoxide and methane over Canada: July–August 1990, *J. Geophys. Res.*, *99*, 1659–1669, 1994b.

Herman, R. L., et al., Measurements of CO in the upper troposphere and lower stratosphere, *Chemosphere Global Change Sci.*, *1*, 173–183, 1999.

Hoor, P., H. Fischer, L. Lange, J. Lelieveld, and D. Brunner, Seasonal variations of a mixing layer in the lowermost stratosphere as identified by the CO-O_3 correlation from in situ measurements, *J. Geophys. Res.*, *107*(D5), 10.1029/2000JD000289, 2002.

Huntrieser, H., H. Schlager, C. Feigl, and H. Höller, Transport and production of NO_x in electrified thunderstorms: Survey of previous studies and new observations at midlatitudes, *J. Geophys. Res.*, *103*, 28,247–28,264, 1998.

Kasischke, E. S., K. Bergen, R. Fennimore, F. Sotelo, G. Stephens, A. Jentos, and H. H. Shugart, Satellite imagery gives clear picture of Russia's boreal forest fires, *Eos Trans. AGU*, *80*, 141, 147, 1999.

Lange, L., Aircraft-borne trace gas measurements during the STREAM 98 campaign, Ph.D. thesis, pp. 53–70, Utrecht Univ., Utrecht, Netherlands, 2001.

Lange, L., et al., Detection of lightning-produced NO in the midlatitude upper troposphere during STREAM 1998, *J. Geophys. Res.*, *106*, 27,777–27,785, 2001.

Lelieveld, J., A. Bregman, H. A. Scheeren, J. Ström, K. S. Carslaw, H. Fischer, P. C. Siegmund, and F. Arnold, Chlorine activation and ozone destruction in the northern lowermost stratosphere, *J. Geophys. Res.*, *104*, 8201–8214, 1999.

Möhler, O., and F. Arnold, Flow reactor and triple quadrupole mass spectrometer investigations of negative ion reactions involving HNO_3: Implications for atmospheric HNO_3 detection by chemical ionization mass spectrometry, *J. Atmos. Chem.*, *13*, 33–61, 1991.

Nakazawa, T., K. Miyashita, S. Aoki, and M. Tanaka, Temporal and spatial variations of upper tropospheric and lower stratospheric carbon dioxide, *Tellus, Ser. B*, *43*, 106–117, 1991.

Parrish, D. D., M. Trainer, J. S. Holloway, J. E. Yee, M. S. Warshawsky, F. C. Fehsenfeld, G. L. Forbes, and J. L. Moody, Relationships between ozone and carbon monoxide at surface sites in the North Atlantic region, *J. Geophys. Res.*, *103*, 13,357–13,376, 1998.

Scheele, M. P., P. C. Siegmund, and P. F. J. v. Velthoven, Sensitivity of trajectories to data resolution and its dependence on the starting point: In or outside a tropopause fold, *Meteorol. Appl.*, *3*, 267–273, 1996.

Schröder, F., and J. Ström, Aircraft measurements of sub micrometer aerosol particles (>7 nm) in the midlatitude free troposphere and tropopause region, *Atmos. Res.*, *44*, 333–356, 1997.

Shipham, M. C., A. S. Bachmeier, D. R. Cahoon Jr., G. L. Gregory, B. E. Anderson, and E. V. Browell, A meteorological interpretation of the Arctic Boundary Layer Expedition (ABLE) 3B flight series, *J. Geophys. Res.*, *99*, 1645–1657, 1994.

Smyth, S., et al., Comparison of free tropospheric western Pacific air mass classification schemes for the PEM-WestA experiment, *J. Geophys. Res.*, *101*, 1743–1762, 1996.

Smyth, S., et al., Characterization of the chemical signatures of air masses observed during the PEM experiments over the western Pacific, *J. Geophys. Res.*, *104*, 16,243–16,254, 1999.

Stohl, A., A one year climatologie of airstreams in the Northern Hemisphere troposphere and lowermost stratosphere, *J. Geophys. Res.*, *106*, 7263–7279, 2001.

Stohl, A., and T. Trickl, A textbook example of long-range transport: Simultaneous observation of ozone maxima of stratospheric and North American origin in the free troposphere over Europe, *J. Geophys. Res.*, *104*, 30,445–30,462, 1999.

Strahan, S. E., A. R. Douglass, J. E. Nielsen, and K. A. Boering, The CO_2 seasonal cycle as a tracer of transport, *J. Geophys. Res.*, *103*, 13,729–13,741, 1998.

Talbot, R. W., et al., Chemical characteristics of continental outflow from Asia to the troposphere over the western Pacific Ocean during September–October 1991: Results from PEM-West A, *J. Geophys. Res.*, *101*, 1713–1725, 1996.

Waibel, A. E., H. Fischer, F. G. Wienhold, P. C. Siegmund, B. Lee, J. Ström, J. Lelieveld, and P. J. Crutzen, Highly elevated carbon monoxide concentrations in the upper troposphere and lowermost stratosphere at northern midlatitudes during the STREAM II summer campaign in 1994, *Chemosphere Global Change Sci.*, *1*, 233–248, 1999.

Warneck, P., *Chemistry of the Natural Atmosphere*, Academic, San Diego, Calif., 1988.

Wernli, H., Lagrangian-based analysis of extratropical cyclones, II, A detailed case study, *Q. J. R. Meteorol. Soc.*, *123*, 1677–1706, 1997.

Wernli, H., and H. C. Davies, Lagrangian-based analysis of extratropical cyclones, I, The method and some applications, *Q. J. R. Meteorol. Soc.*, *123*, 467–489, 1997.

Wienhold, F. G., et al, TRISTAR: A tracer in-situ TDLAS for atmospheric research, *Appl. Phys. B*, *67*, 411–417, 1998.

Wofsy, S. C., S.-M. Fan, D. R. Blake, J. D. Bradshaw, S. T. Sandholm, H. B. Singh, G. W. Sachse, and R. C. Harriss, Factors influencing atmospheric composition over subarctic North America, *J. Geophys. Res.*, *99*, 1887–1897, 1994.

Wotawa, G., and M. Trainer, The influence of Canadian forest fires on pollutant concentrations in the United States, *Science*, *288*, 324–328, 2000.

Zöger, M., et al., Fast in situ stratospheric hygrometers: A new family of balloon-borne and airborne Lyman α photofragment fluorescence hygrometers, *J. Geophys. Res.*, *104*, 1807–1816, 1999.

D. Brunner and H. Wernli, Institute for Atmospheric Science, ETH Hönggerberg HPP, Swiss Federal Institute of Technology, Zürich, CH-8093 Switzerland. (dominik.brunner@atmos.umnw.ethz.ch; henry@atmos.umnw. ethz.ch)

H. Fischer, P. Hoor, J. Lelieveld, J. Williams, and S. Wong, Max Planck Institute for Chemistry, P. O. Box 3060, D-55020 Mainz, Germany. (hofi@mpch-mainz.mpg.de; hoor@mpch-mainz.mpg.de; lelieveld@mpch-mainz.mpg.de; williams@mpch-mainz.mpg.de; wong@mpch-mainz.mpg.de)

G. W. Harris and J. Rudolph, Centre for Atmospheric Chemistry, York University, 4700 Keele Street, North York, Ontario, Canada M3J 1P3. (gharris@turing.sci.yorku.ca; rudolphj@yorku.ca)

D. S. McKenna, National Center for Atmospheric Research, 1850 Table Mesa Drive, Boulder, CO 80307-3000, USA. (danny@ucar.edu)

H. A. Scheeren, Institute for Marine and Atmospheric Research, Utrecht University, Princetonplein 5, NL-3584 CC Utrecht, Netherlands. (h.a.scheeren@fys.ruu.nl)

P. Siegmund, Royal Netherlands Meteorological Institute, Postbus 201, AE DeBilt, NL-3730 Netherlands. (siegmund@knmi.nl)

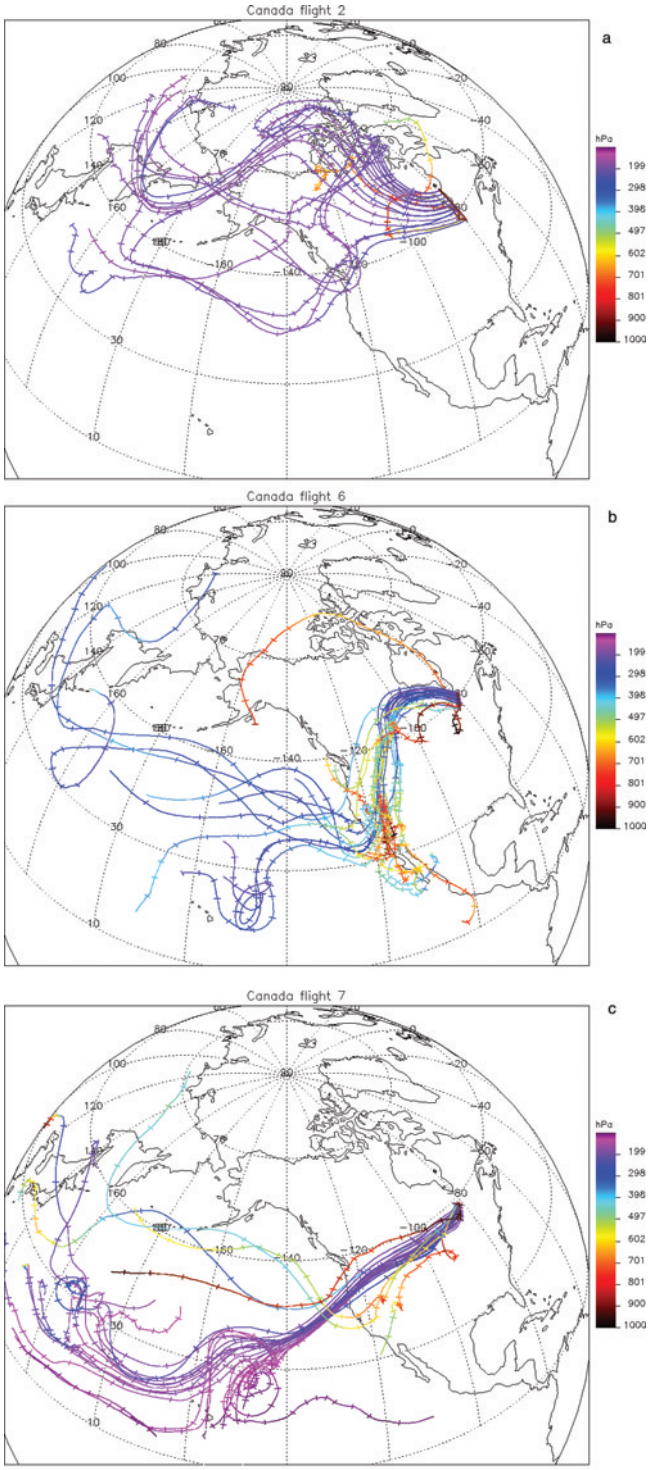

Figure 2. Ten day back trajectories for (a) a polar (STR-2), (b) a midlatitudinal (STR-6), and (c) a (sub)tropical (STR-7) air mass origin. Ticks indicate 12 hour intervals, while the color code indicates the pressure in hectopascals.

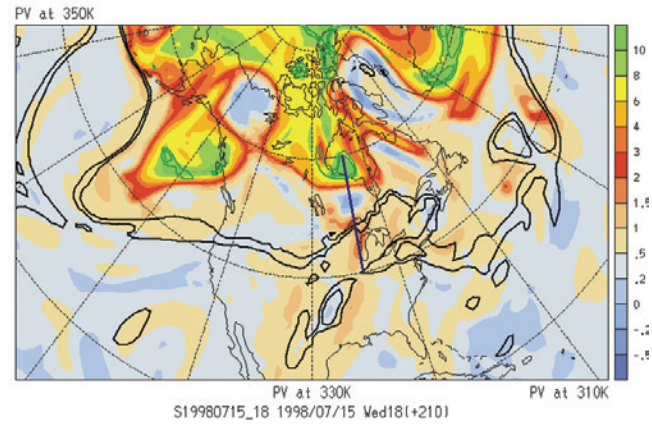

Figure 7. Analysis of the potential vorticity at the 330 K level for 15 July, 1800 UTC. Superimposed are the PV = 2 and PV = 3 lines at 350 K (black lines) and 310 K (green lines). The black lines mark the position of the subtropical jet at 350 K, while the colored contours at 2–3 PVU indicate the position of the polar jet at 330 K. The blue line is the horizontal projection of the vertical cross section shown in Figure 8.

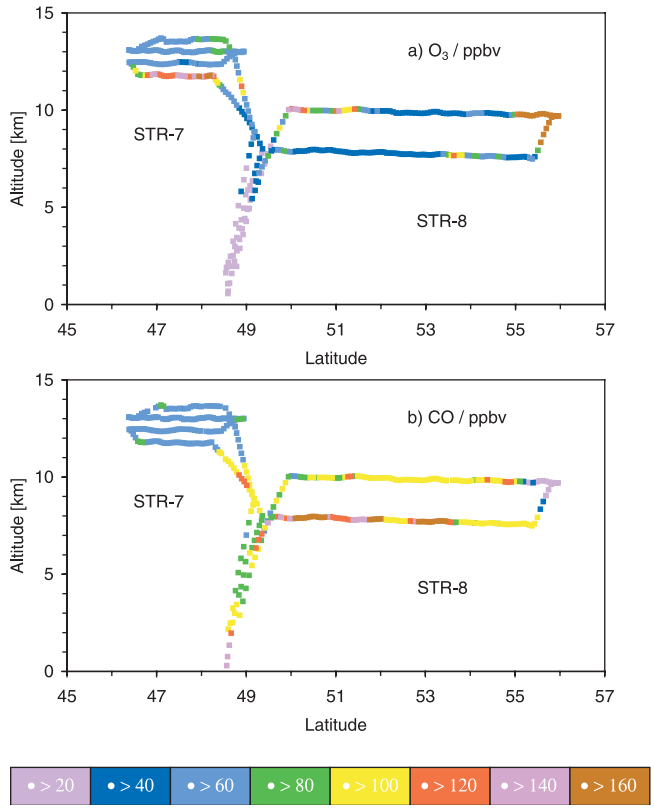

Figure 10. Latitude-altitude plot of the (a) O_3 and (b) CO concentrations during STR-7 and STR-8, ahead and behind a surface cold front. The data points colored in brown indicate mixing ratios in excess of 160 ppbv for O_3 and CO, respectively.